Enhanced removal of amoxicillin and chlorophenol as a model of wastewater pollutants using hydrogel nanocomposite: Optimization, thermodynamic, and isotherm studies

Aseel M. Aljeboree[*1], **Zainab D. Alhattab**[2], **Usama S. Altimari**[3], **Ahmed Kareem Obaid Aldulaim**[4], **Asmaa Kefah Mahdi**[5], **Ayad F. Alkaim**[1]

1. Department of Chemistry, College of Sciences for W, University of Babylon, Hilla, Iraq
2. Ministry of Interior Affairs, Babylon Police Command, Criminal Evidence Investigation Department, Iraq
3. Department of Medical Laboratories Technology, AL-Nisour University College, Baghdad, Iraq
4. Department of Pharmacy, Al-Zahrawi University College, Karbala, Iraq
5. National University of Science and Technology, Dhi Qar, Iraq

*Corresponding author's Email: annenayad@gmail.com

ABSTRACT

Studies have been conducted to gain understandings and generic knowledge of the equilibrium aspects of adsorption of different adsorbents, SA-Bn-TiO$_2$ NPs surfaces. Removal of two pollutants, Amoxicillin drug AMX, 4-chlorophenol (CPH) from aqueous solutions by adsorption with SA-Bn-TiO$_2$ NPs, SA-Bn and TiO$_2$ NPs surfaces were experimentally determined. The best results were found at pH 6.6, temperature 30 ℃, and adsorbent dosage of 0.05 g of SA-Bn-TiO$_2$ NPs for both studying adsorption capacity and removal percentage. The morphology and structure of the SA-Bn-TiO$_2$ NPs hydrogel beads were investigated utilizing Ultraviolet-Visible Spectroscopy (UV–Vis), Fourier Transform Infrared (FT-IR), Thermo gravimetric analysis (TGA), Field Emission Scanning Electron Microscopy (FE-SEM), Transmission Electron Microscopy (TEM), Energy Dispersive X-Ray (EDX) and X-ray Diffraction Spectroscopy (XRD). The best contact time for equilibrium reached one hour. It is essentially due to saturation of the active site which does not let further adsorption to take place. For the two pollutants onto hydrogel, best adsorption was found to be at pH 11, and adsorption raised by increase in the pH solution. The value negative of ΔG confirmed that the nature adsorption process is spontaneous. The value positive of ΔS confirmed the raise randomness at the solid-solution interface pending adsorption and the value positive of ΔH confirmed that adsorption process is endothermic.

INTRODUCTION

Hydrogels are polymer chains that are highly hydrophilic, so that they are cross-linked to form hydrogels that have a high ability to swell in an aqueous solution, and their characteristics are that they trap pollutants inside them for the longest possible period without dissolving. It also contains carboxylic, imide, amine, hydroxyl, and sulfonyl groups in its three-dimensional structure. These groups are hydrophilic and also have the ability to swell (Dhiman *et al.* 2020). Depending on the nature hydrogel, it can be classified. Establishing on several properties can be based on if they are natural (biopolymers) or synthetic (utilize of synthetic monomers), a mixing of natural and synthetic to give a hybrid hydrogel (Jawad & Radia 2021; Malatji *et al.* 2021). Amoxicillin (AMX) is a semi-synthetic β-lactam antibiotic belonging to the group of penicillin (Fig. 1) consists of d-4-hydroxyphenylglycine side chain linked to 6-aminopenicillanic acid (6-APA) moiety. This molecule is relatively unstable both in aqueous solution and storage. Amoxicillin (AMX) have been widely utilized in human and

veterinary medicine for the treatment of bacterial infections caused via Gram-positive and Gram-negative organisms (Aljeboree *et al.* 2019; Moussavi *et al.* 2020;). However, AMX can cause some side-effects on human beings as other β-lactam antibiotics. Various preparations of this drug either alone or combined with other ingredients are commercially available (Alqaragully *et al.* 2015; Karimi Maleh & Tahernejad Javazmi 2020). It can cause serious pollution problems. 4-Chlorophenol (called also as p-Chlorophenol) is an organic compound and one of three monochlorophenol isomers. Chemical formula: ClC_6H_4OH, molar: mass 128.56 g mol^{-1}, colourless or white solid that melts easily and exhibits significant solubility in water (Pozan 2014; Jun *et al.* 2019 Gulin Selda) as shown in Fig. 1.
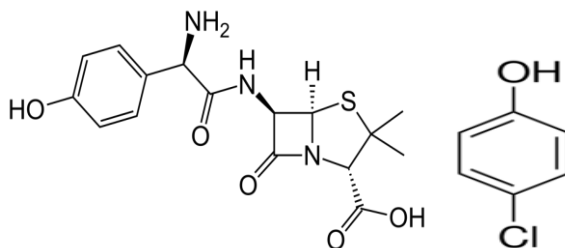

**Fig. 1.** Chemical structure of Amoxicillin (AMX) and 4-Chlorophenol (CPH).

MATERIALS AND METHODS

Materials

Bentonite clay, Sodium alginate (SA), Calcium chloride dehydrate ($CaCl_2$-2H_2O), and Titanium (IV)- bis (ammonium lactate) dihydroxide (TALH) solution were supplied by Sigma–Aldrich.

### Preparation of the Titanium dioxide nanoparticles

Titanium dioxide nanoparticles were prepared by the Hydrothermal method of titanium (IV) bis (ammonium lactate) di-hydroxide (TALH). This experiment was carried out in a 250-mL Teflon cup, adding 10 mL of (TALH) aqueous solution. The concentration of 0.1 M ammonium hydroxide (NH_4OH) wear mixed, followed via the addition of DW to reach l volume of 100 mL as appear in Scheme 1.
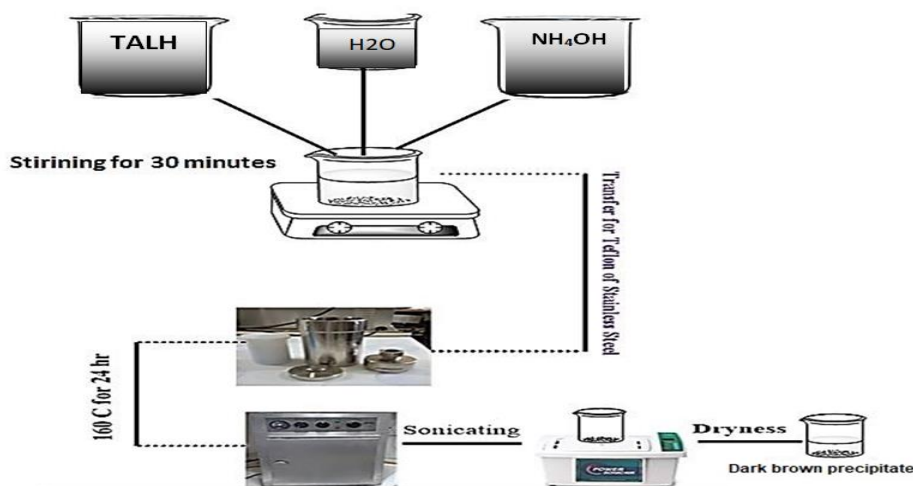
Scheme 1. Preparation of TiO_2 nanoparticles.

Preparation of hydrogel beads

Preparation of SA-Bn-TiO_2 NPs was carried out based on sodium alginate (SA) by dissolving 4 g SA in 150 mL DW and stirring at 350 rpm for 2 hours. At the same time, 2 g bentonite clay was dissolved in 50 mL DW. After one hour of reaction time, the slurry solution was added to the sodium alginate (SA) solution gradually until a homogeneous solution and a well-dispersed hydrogel were formed. The second stage was to add the homogeneous solution obtained from a syringe needle by dropping into a bath saturated with a mixed solution of TiO_2 NPs 0.5% (w/v) and $CaCl_2$.2H_2O 6% (w/v) and impregnation of its surface with TiO_2 NPs (shown image of hydrogel in Fig. 2).
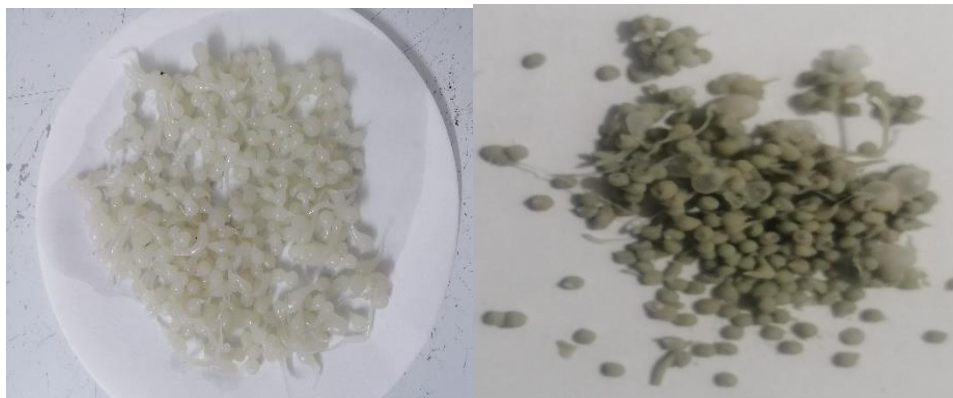
Photo 1. Preparation of hydrogel beads.

Effect of several factors on the adsorption methods
Effect of Initial Concentration of pollutant
A series of several concentrations of 100 mL for pollutant has been used in this study. A total of 10-100 mg L^{-1}, was added to Erlenmeyer flask in 0.05 g/100 mL of SA-Bn-TiO$_2$ NPs at 30 °C and 220 rpm shaking speed these series were putting for 1 hr in a shaker water bath. The adsorption capacity was calculated from equation 1 (Tariq *et al.* 2021):

$$qe = \frac{(C_0 - C_e) * V_L}{m_{gm}} \qquad (1)$$

The removal rate of E (%) of the pollutant was calculated from equation 2 (Zhao Ying *et al.* 2020)

$$E \% = \frac{C_0 - C_e}{C_0} * 100 \qquad (2)$$

Effect of dose of adsorbent
The study was carried out with several doses (0.02, 0.03, 0.05, 0.08, and 0.1 g) for SA-Bn-TiO$_2$ NPs. The concentrations pollutant were 100 mg L^{-1}. The solutions were put in the shaker water bath about 1 h at 30 ℃.

Effect of pH
The influence of pH solution on the pollutant removal was examined by varying the initial solution pH (4, 5, 6, 8, and 10) using conical flasks (100 mL) container concentrations (100 mg L^{-1}) in 100 mL. The pH was adjusted via utilizing 0.1 N HCl and/or 0.1 N NaOH and was measured by a pH meter. Then the quantity of adsorbent (0.05 g/100 mL) of SA-Bn-TiO$_2$ NPs adsorbents was set on the conical flask. The flasks were placed inside the shaker water bath maintained at 30 ℃ and the final concentration of dye was measured using the single beam UV-Vis spectrophotometer.

Effect of solution Temperature
The adsorption experiments were performed at several temperatures (10-40 °C) in a thermostat water bath with a shaker. The influence of solution temperature was examined with 0.05 g dose of adsorbent SA-Bn-TiO$_2$ NPs mixing with 100 mL aqueous solution of pollutant concentration (10-100 mg L^{-1}), and the sample was shaking at a period for 1 h. Then the remaining pollutant concentration in the aqueous phase was measured spectrophotometrically for the chosen wavelength.

Amoxicillin drug loading
About 0.5 g SA-Bn-TiO$_2$ NPs was added to 100 mL amoxicillin solution in concentration of 500 mg L^{-1} and placed in a shaker device for a period of 1 h at 30 ℃, afterward the surface was separated from the solution and the drug-loading SA-Bn-TiO$_2$ NPs was dried in an oven at 70 ℃ and then ground to obtain the powder.

***In vitro* drug release**
The effect of the hydrogel loaded with a drug in different acidic media, as the release of the drug at pH 1.2 and pH 7.5 was studied. An amount of 0.1 g of the surface loaded by a drug was placed in 100 mL of different acidic

media, then placed in a shaker water bath at 37 ℃ in different times. The removal percentage and amount of drug release is calculated through the equations.

$$\text{Amount of drug release} = \frac{C_e \, V}{M} \qquad (3)$$

$$\text{Drug release (\%)} = \frac{\text{amount of drug release}}{\text{amount of drug loading}} \times 100 \qquad (4)$$

RESULTS AND DISCUSSION
Physicochemical characterization of adsorbents surfaces

FT-IR technique was utilized to analyse the surface functional groups responsible for two pollutant (AMX and CPH) adsorption. Adsorbent surfaces of SA-Bn-TiO$_2$NPs and pollutant-loaded adsorbent samples after adsorption was placed in an oven at 65 ℃ for 4 h. Results shown in Fig. 2 exhibit the FT-IR spectra of the SA-Bn and SA-Bn-TiO$_2$. Starting by the SA-Bn, it clears that the characteristic bands of the polymer matrix are well depicted at 3300 cm^{-1}, 1600 cm^{-1}, and 1409 cm^{-1} assigned respectively to the stretching vibration of –O–H from the OH group, to C=O, and to symmetric COO$^-$ stretching vibrations. New characteristic adsorption band 1718 cm^{-1}, assigned to C=O stretching in the spectrum of SA-Bn-TiO$_2$. Also teeth like peaks in the region about 450-600 cm^{-1} of Ti-O bending are observed which confirms the impregnation of TiO$_2$ NPs (Zhao Ying *et al.* 2020; Soulaima Chkirid *et al.* 2021) .
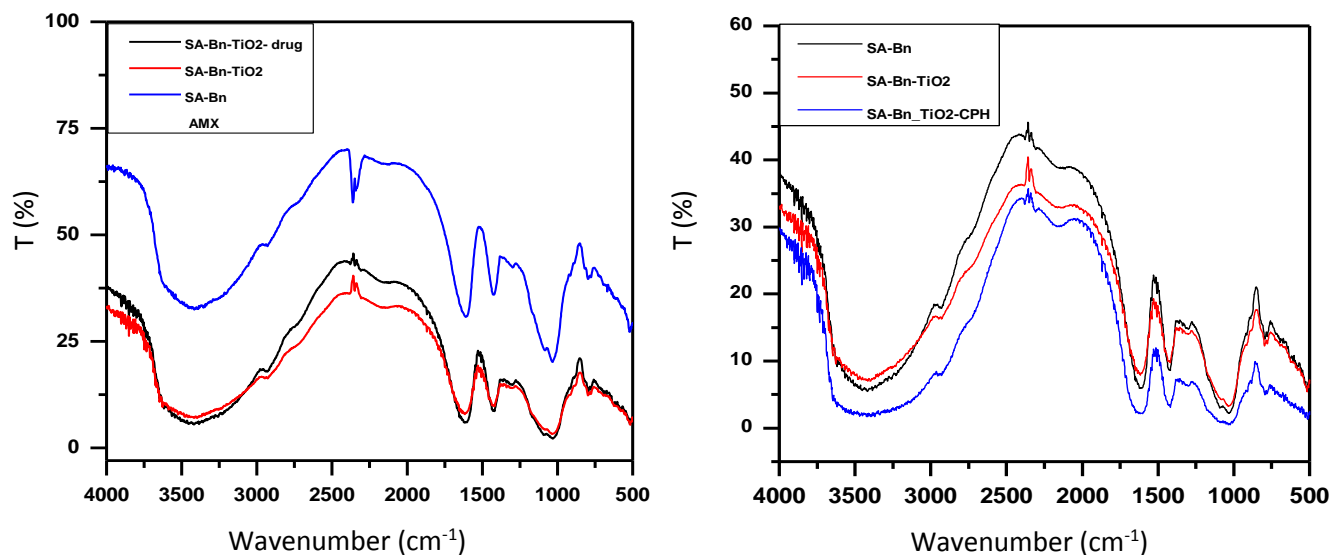

Fig. 2. FT-IR spectra of SA-Bn-TiO$_2$ NPs surface before, and after adsorption of AMX and CPH.

FE-SEM was utilized to study the morphology of hydrogel before and after AMM and CPH adsorption as shown in Fig. 3a: bentunite clay; c) SA-Bn; d) SA-Bn-TiO$_2$. The surface morphology of SA-Bn is found to be smooth (Fig. 4b), whereas, after grafting of SA-Bn on TiO$_2$ NPs, the surface morphology becomes rougher displayed the existence of holes and cavities with different sizes and shapes (Hemant Mittal *et al.* 2021; Fig. 3c). The internal pores can be observed in the morphology of SA-Bn-TiO$_2$ NPs, which favours the intraparticle diffusion of two pollutant as shown in Figs. 3d and 3e. TiO$_2$ NPs were sufficient to create well-developed pores with uniform distribution leading to large surface area and porous structure. The pores and surface of SA-Bn-TiO$_2$ NPs hydrogel were entirely occupied. Furthermore, this confirms the adsorption of the two pollutants by SA-Bn-TiO$_2$ NPs (Mittal 2019). Fig. 3f shows image of TEM SA-Bn-TiO$_2$ NPs, where TiO$_2$ NPs was observed embedded inside the SA-Bn-TiO$_2$ NPs hydrogel.
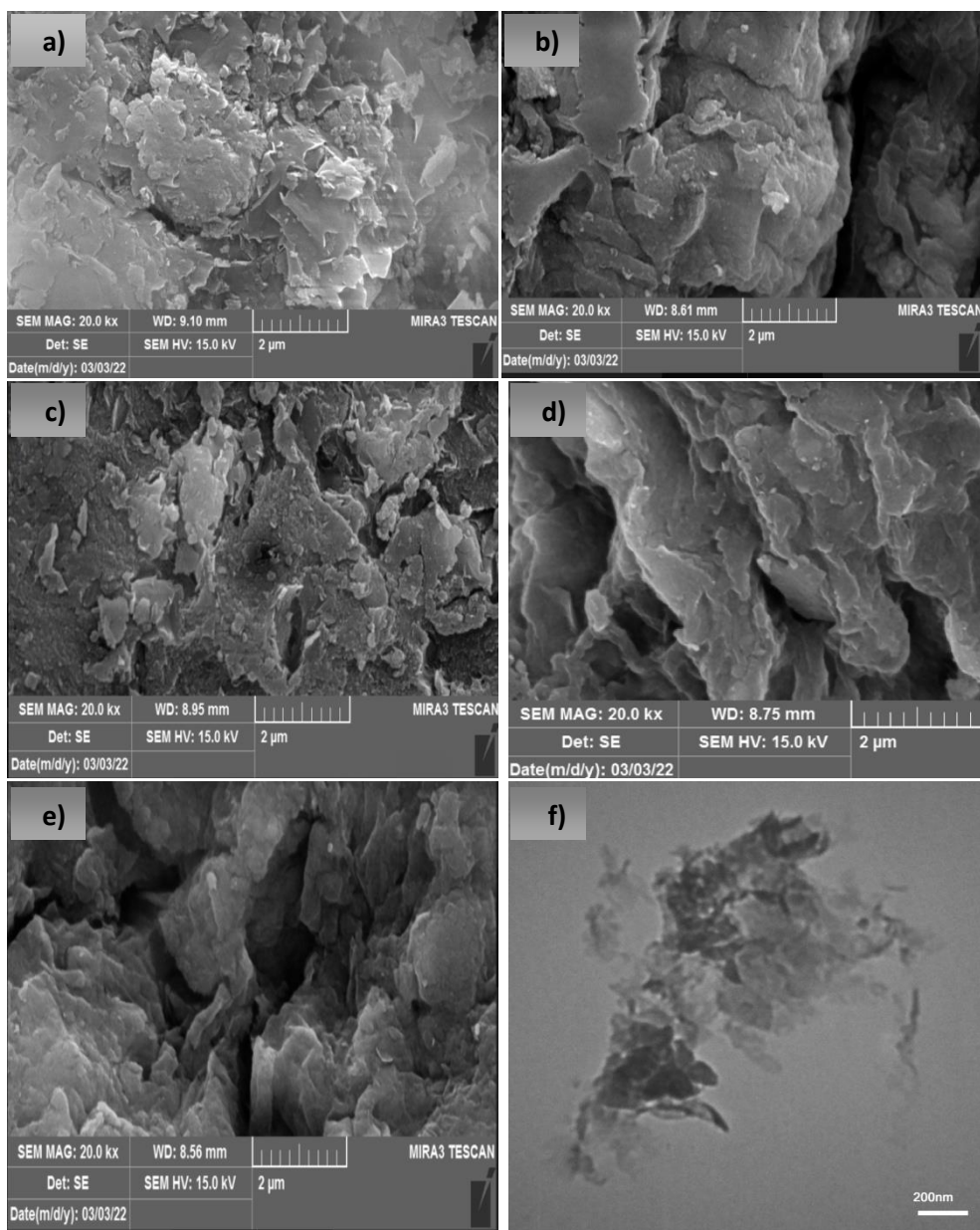
Fig. 3. Images of FE-SEM (a) Clay Bentonite; (b) SA-Bn; (c) SA-Bn-TiO$_2$ NPs; (d) AMX loaded SA-Bn-TiO$_2$ NPs; and (e) CPH loaded SA-Bn-TiO$_2$ NPs and TEM images of a) SA-Bn-TiO$_2$ NPs.

Adsorbent mass of nanocomposite

The influence of the quantity of the adsorbents was necessary to observe the minimum probable quantity, which shows the maximum adsorption stoichiometric. The quantities of the adsorbent varied from 0.02 to 0.1 g/100 mL of SA-Bn-TiO$_2$ NPs (Fig. 5). An increase in the E (%) of the pollutants (AMX and CPH) removal with mass of adsorbent was related to rises in the adsorbent surface areas and improving the number of adsorption sites obtainable for adsorption as reported already in other cases. The rise in removal of pollutants (AMX and CPH) with mass of nanocomposite due to the introduction of more binding sites for adsorption (Yasin *et al.* 202; Alkaim & Ajobree 2020). The primary parameter explaining this characteristic is that adsorption sites remain un-saturated during the adsorption reaction, whereas the number of sites available for adsorption site rises via increasing the adsorbent amount (Qiuyan *et al.* 2022; Al Niaeem & Whidad Hanoosh 2022).

Effect of solution pH

The effect of pH on the adsorption of pollutants AMX and CPH onto SA-Bn-TiO$_2$ NPs was studied at a pH solution choice of 3-10 in the presence of primary concentrations (100 mg L^{-1}; Fig. 6). The equilibrium sorption capacity of AMX and CPH on SA-Bn-TiO$_2$ NPs was very little at pH 3 (56.310 mg g^{-1}, 77.45mg g^{-1} respectively

which suggests that SA-Bn-TiO$_2$ NPs are excellent adsorbents for pollutant removal from large volumes of aqueous solutions (Jiang *et al.* 2019; Aljeboree & Alkaim 2019).
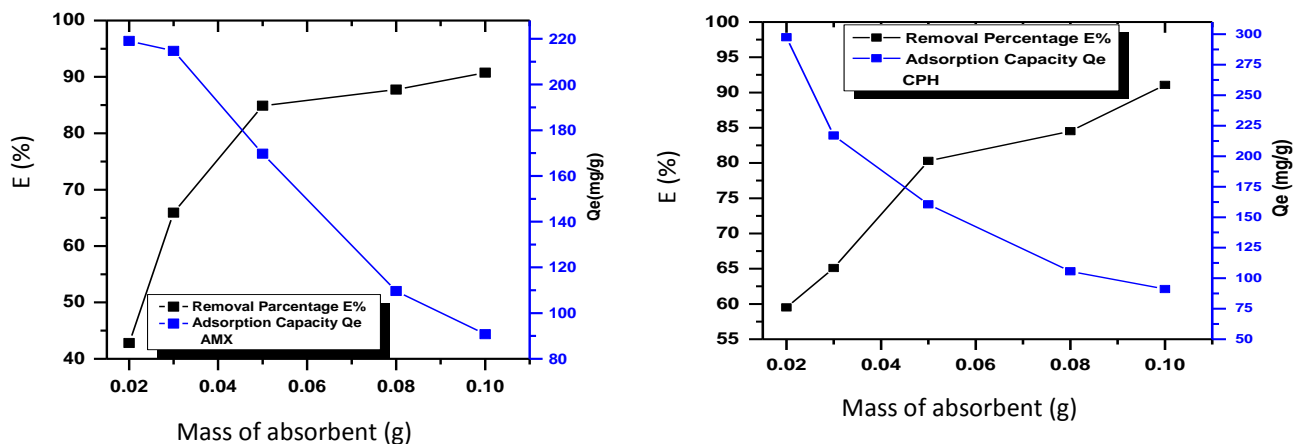
Fig. 4. Effect of the mass quantity of adsorbent SA-Bn-TiO$_2$ NPs on the percent removal and quantity of adsorbed AMX and CPH.

When the pH is higher than 6, the sorption capacity of pollutant on SA-Bn-TiO$_2$ NPs increases by elevating pH values (Fig. 6). The removal of three pollutants from aqueous solution by SA-Bn-TiO$_2$ NPs is highly pH-dependent. The results exhibited the maximum adsorption of the pollutants (AMX and CPH) between pH 6-10. The adsorption capacity (qe) upraises by elevating pH. Lower adsorption at acidic pH may be due to the presence of excess ions H+ competing with the cation groups on the pollutants for adsorption sites. At higher pH, the surface may get charge positively, which improves the negatively charged the pollutants anions through electrostatic forces of attraction (Yu *et al.* 2019; Aljeboree *et al.* 2019).

Effect of temperature

To determine whether the ongoing adsorption method was exothermic or endothermic, the adsorption isotherms were estimated for several pollutants-adsorbent ways. The removal of AMX and CPH has been studied at different temperatures (283.15, 293.15, 303.15 and 313.15 K) in the presence of various initial concentrations (10-100 mg L^{-1}; Fig. 7). The data appear that the equilibrium adsorption efficiency of AMX and CPH were upraised, while elevating the temperature solution for totally primary concentrations. As observed from Fig. 7, the uptake capacity of SA-Bn-TiO$_2$ NPs increases by rising temperature, due to the improved magnitude of the reverse (desorption) step in the mechanism. This is probably due to the endothermic effect of the surroundings during the adsorption method (Kamil *et al.* 2016; Alshamri & Mohammed 2021).

Effects of temperature on adsorption will also help in the calculation of the basic thermo-dynamic parameter like (ΔG), (ΔH), and (ΔS) of the adsorption method. The (K$_e$) of the adsorption method at each temperature, was obtained from the equation 5:

$$K_e = \frac{(Q_{max}) * Wt\ (0.05\ g)}{(C_e) * V (0.1L)} \qquad (5)$$

where Q$_{max}$ is the quantity adsorbed in mg g^{-1}, C$_e$ is the equilibrium concentration (mg L^{-1}) of 0.05 g mass of the SA-Bn-TiO$_2$ NPs adsorbent, and 0.1 L volume of pollutant (AMX, CPH) solution utilized in the adsorption method (Al Niaeem & Hanoosh 2022). The ΔG could be calculate from the equation 6: Al Niaeem & Hanoosh 2022):
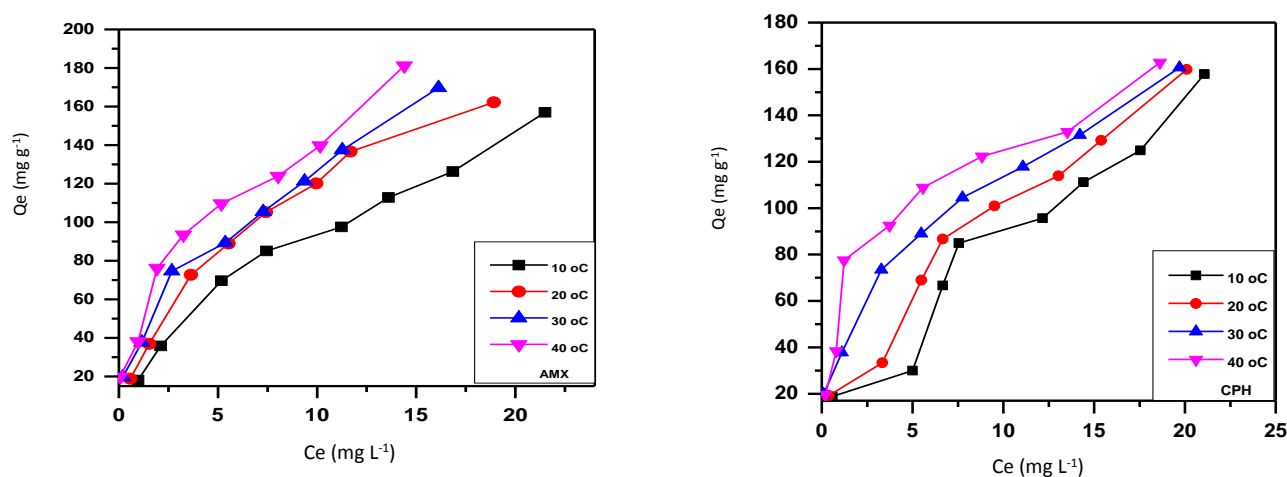
$$ΔG = -RT \ln K_e \qquad (6)$$

where $ΔG$: Gibbs free energy (J.K^{-1} mol^{-1}), R / gas constant (8.314 J.K^{-1} mole^{-1}), T / temperature in Kelvin. The $ΔH$ of adsorption may be calculate equation 7 (Osman & Saleh 2020):

$$\ln X_m = -\frac{ΔH^°}{RT} + Cons. \qquad (7)$$
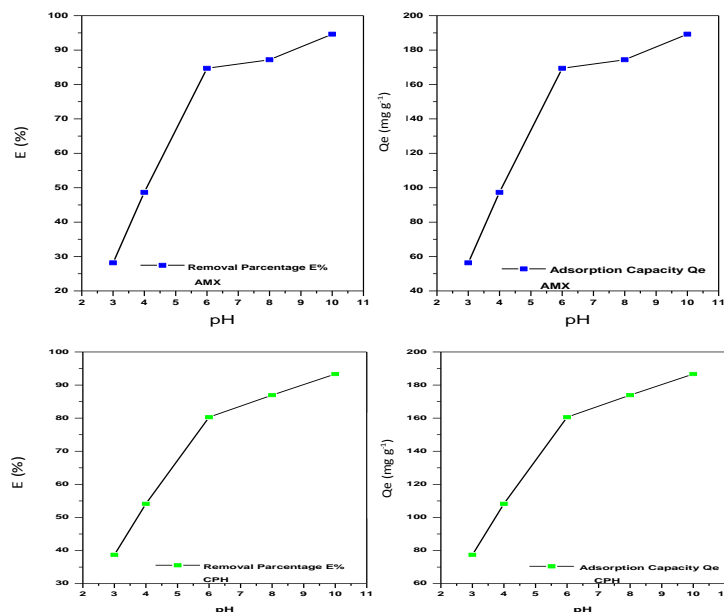
Fig. 5. Effect of solution pH on the adsorption of AMX and CPH on SA-Bn-TiO$_2$ NPs (Exp. Condition: Temp. = 30 °C, contact time 1 h, and pH of solution 6.6).

Fig. 6. Effect of temperature on the adsorption of AMX and CPH on the surface of SA-Bn-TiO$_2$ NPs.

Plotting lnX$_m$ versus 1/T should produce a straight line with a slope -ΔH/R (Fig. 8). The value of ΔS can be obtained from the slope and intercept respectively (Nasseh *et al.* 2019). From data in Table 1, the ΔH and ΔS for adsorption are assumed to be temperature in-dependent. The ΔH is a measure of the energy barrier that should be overcome via reacting molecules (Zhao *et al.* 2020; Sakin *et al.* 2019)

Comparative adsorption between several surfaces to remove AMX and CPH

A comparative study between titanium dioxide (TiO$_2$), Sodium alginate-bentonite (SA-Bn), sodium alginate-bentonite-titanium dioxide (SA-Bn-TiO$_2$ NPs) surfaces as adsorbents were carried out. A sample of 100 mL of AMX and CPH concentrations (100 mg L^{-1}) were used in this study, then were added to Erlenmeyer flask using 0.05 g titanium dioxide (TiO$_2$), sodium alginate-bentonite (SA-Bn), sodium alginate- bentonite-titanium dioxide (SA-Bn-TiO$_2$ NPs), and were placed in a shaker water bath for one hour. Afterward, the supernatant was separated by centrifuge and measured the remaining concentration by UV-visible at the λ max (nm; Xiong *et al.* 2020). The best results of the percentage of removal (E%) for AMX and CPH based on the ascending order were: SA-Bn-TiO$_2$ NPs > SA-Bn > TiO$_2$ NPs (Fig. 8).
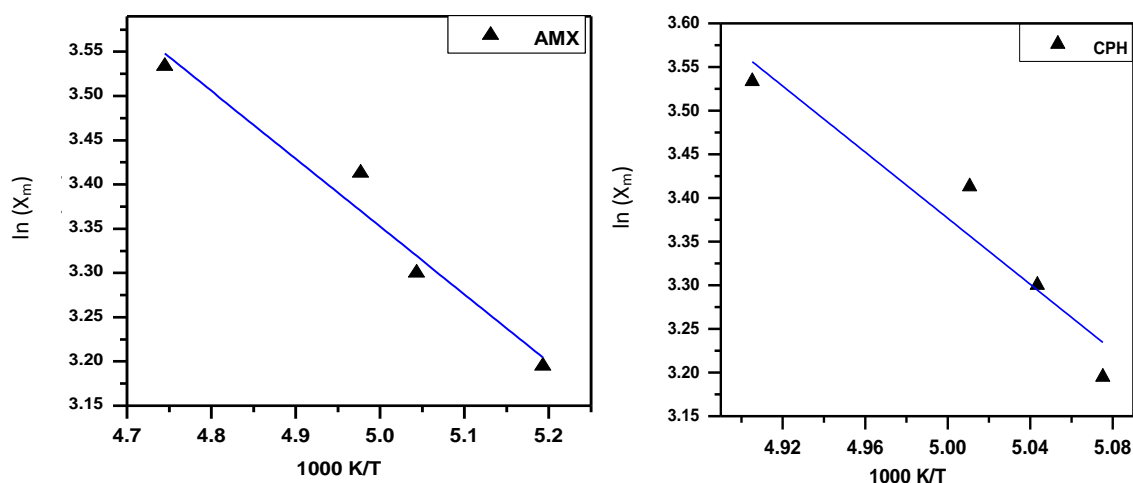
Fig. 7. Plot ln X_m against the absolute temperature of the adsorption of AMX and CPH onto SA-Bn-TiO2 NPs.

Table 1. Thermodynamic parameter ΔS, ΔG and ΔH of AMX and CPH adsorbed onto SA-Bn-TiO2 NPs.

SA-Bn-TiO2 NPs adsorbent/ AMX adsorbate

Thermodynamics parameters T/K	K_e	$-\Delta G^\circ$/ kJ mol^{-1}	ΔH°/ kJ mol^{-1}	ΔS°/ J.K^{-1} mol^{-1}
283.15	8041.95	21.157		
293.15	22307.69	24.390		
303.15	23846.15	25.391	10.424	76.563
313.15	27692.31	26.618		

SA-Bn-TiO2 NPs adsorbent/ CPH adsorbate

| Thermodynamics parameters T/K	K_e	$-\Delta G^\circ$/ kJ mol^{-1}	ΔH°/ kJ mol^{-1}	ΔS°/ JK^{-1} mol^{-1}
283.15	7105.263	20.8666		
293.15	7894.737	21.8606		
303.15	8157.895	22.6893	4.029	55.1816
313.15	8421.055	23.5207		

Effect of pH on releasing ratio of amoxicillin *in vitro*

The release of amoxicillin was studied in conditions similar to the human body in terms of acidity and temperature. It was found that the speed of amoxicillin release was higher when the acidity function (pH 7.5). This is due to the degree of swelling of the hydrogel and the dissolution of amoxicillin which depends on the acidity function. The speed of release of amoxicillin in the alkaline medium as a result of elevation in the rate of swelling was more than in the acidic medium (Kevadiya *et al.* 2021). In the case of acidic function (pH 1.2), the concentration of H$^+$ upraises, which competes with the unlinked amino group. Thus, the percentage of hydrogel swelling declines, and also the percentage of drug release decreases. The initial burst release of 42% and 25%, in the first one hour was

observed for AMX. The cumulative release of AMX in three hours was 68% and 44% at pH 7.5 and pH 1.2 respectively (Kevadiya *et al.* 2021; Aguzzi *et al.* 2020), as shown in Fig. 3 (Bhavesh *et al.* 2021).
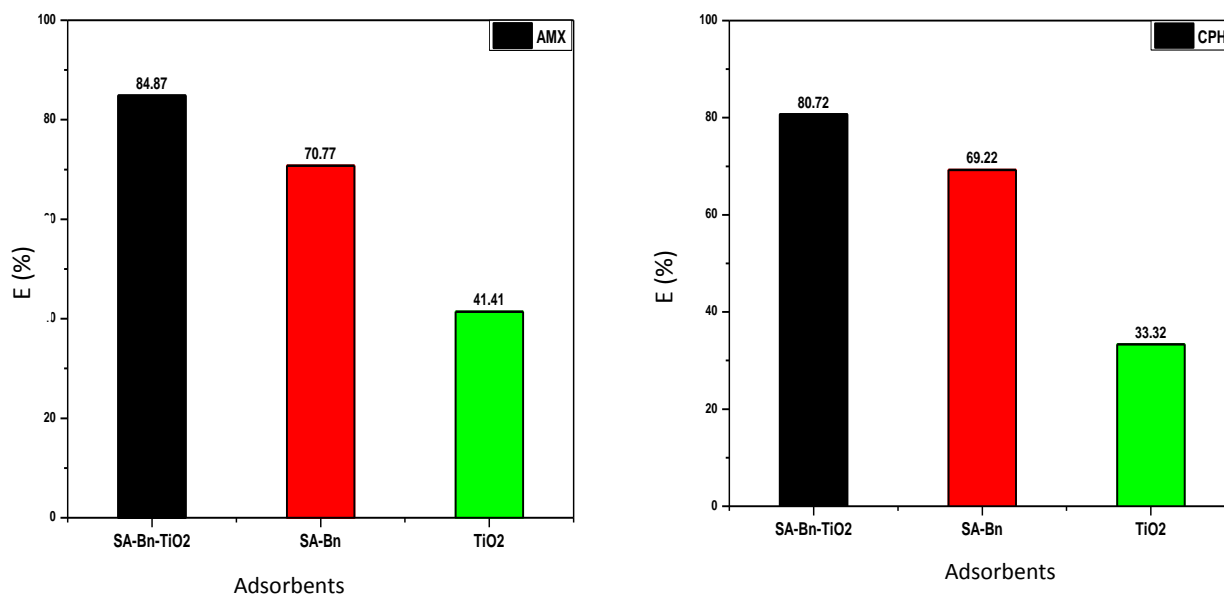
Fig. 8. Comparative adsorption between several surfaces to remove AMX and CPH.
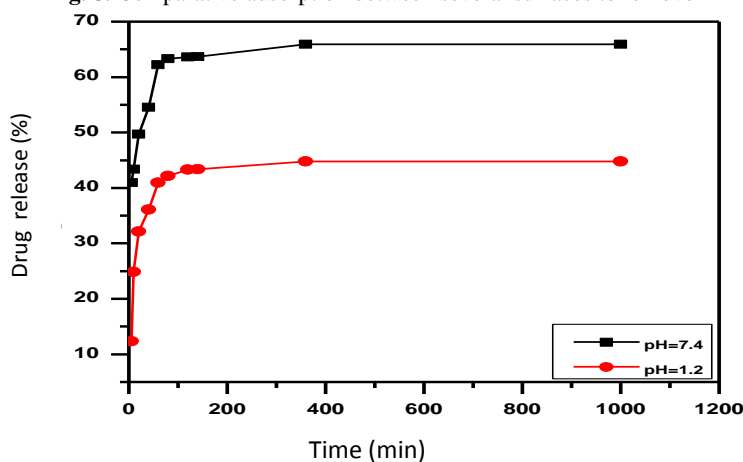
Fig. 9. Drug Release profiles of AMX from the SA-Bn-TiO₂ NPs at pH 1.2 and pH 7.4 (Temperature: 37 °C).

Adsorption Isotherms

The Freundlich isotherm is defined through the following equation 8 (Freundlich 1939):

$$q_e = K_f C_e^{1/n} \qquad (8)$$

where qe: Quantity adsorbed per unit mass of adsorbent at equilibrium (mg g^{-1}) and (mol g^{-1}); Ce: equilibrium concentration (mg L^{-1}) and (mol L^{-1}); K$_f$: Empirical Freundlich constant or efficiency parameter (L/mg) or the pollutant amount adsorbed for unit equilibrium concentration, 1/n: Freundlich exponent (Liu *et al.* 2019; Kim & Jin Hyun 2019). The Langmuir model is mostly utilized for pollutants adsorption from liquid solutions. The nature of the adsorption process was derived by Langmuir alternative equation 9 (Langmuir 1918; Zaheer *et al.* 2019):

$$q_e = \frac{q_m K_L C_e}{1 + K_L C_e} \tag{9}$$

A plot of q_e versus C_e (Figs. 9 & 10) where the values of K_F and $1/n$ are obtained from the intercept and slope of the linear regressions. The correlation coefficient (R^2 values) for the isotherm Freundlich at 30 °C were $R^2 =$

0.9998, $R^2 = 0.9879$ and $R^2 = 0.9988$ of CR, AMX and CPH onto SA-Bn-TiO$_2$ NPs respectively (Kumar *et al.* 2019).
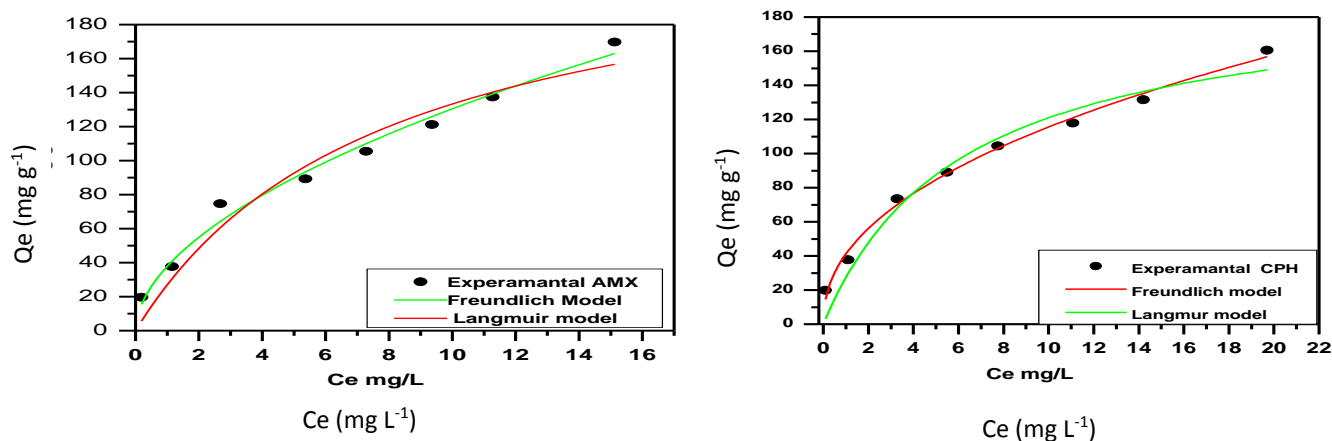

Fig. 10. Several adsorptions nonlinear models fit of adsorption AMX and CPH onto SA-Bn-TiO$_2$.

CONCLUSION

The results of the adsorption study show that percentage removal increases by the elevation in the weight of the surfaces, while the contact time and optimized value of agitation time is 1 h. The release of amoxicillin was studied in conditions similar to the human body in terms of acidity and temperature. Drug release of 62% and 42%, in the first 1 h was observed for AMX. The cumulative release of AMX in three hours was 68%, 44% from pH 7.5 and pH 1.2 respectively. The interaction among quantity and primary concentration showed a significant effect on the adsorption. Adsorbent showed fits best model Freundlich which suggests that adsorption is heterogeneous. The adsorption efficiency for removal of the two pollutants by SA-Bn-TiO$_2$ NPs surface was found to be better than the SA-Bn and TiO$_2$ NPs.

REFERENCES

Aguzzi, C, Capra, P, Bonferoni, C, Cerezo, P, Salcedo, I, Snchez, R, Caramella, C & Viseras, C 2020, Chitosanâ silicate biocomposites to be used in modified drug release of 5-aminosalicylic acid (5-ASA). *Applied Clay Science*, 50: 106-111.

Al Niaeem, HS & Hanoosh, W 2022, Preparation of semi ipns-hydrogel composite for removing congo red and bismarck brown y from wastewater: kinetic and thermodynamic study. *Egyptian Journal of Chemistry*, 56: 19-34.

Aljeboree, AM & Alkaim, AF 2019, Role of plant wastes as an eco-friendly for pollutants (crystal violet dye) removal from aqueous solutions. *Plant Archives*, 19: 902-905.

Aljeboree, AM, Alshirifi, AN & Alkaim, AF 2019, Activated carbon (as a waste plant sources)-clay micro/nanocomposite as effective adsorbent: Process optimization for ultrasound-assisted adsorption removal of amoxicillin drug. *Plant Archives*, 19: 915-919.

Aljeboree, AM, *et al.* 2019, Photocatalytic degradation of textile dye crystal violet wastewater using zinc oxide as a model of pharmaceutical threat reductions. *Journal of Global Pharma Technology*, 11:138-143.

Alkaim, AF & Ajobree, AM 2020, White marble as an alternative surface for removal of toxic dyes (Methylene blue) from Aqueous solutions. *International Journal of Advanced Science and Technology*, 29: 5470-5479.

Alqaragully, MB *et al.* 2015, Monoethanolamine: Production plant. *Research Journal of Pharmaceutical, Biological and Chemical Sciences*, 6: 1287-1296.

Amer, M, Alshamri, AM, Alqaragully, MB & Alkaim, AF 2021, Removal of toxic textile dyes from aqueous solution through adsorption onto coconut husk waste: Thermodynamic and isotherm studies. *Caspian Journal of Environmental Sciences*, 19: 513-522

Chkirid, S, Zari, N, Achour, R, Hassoune, H, Lacheha, A, Qaiss, AeL & Bouhfid, R, Highly synergic adsorption/photocatalytic efficiency of Alginate/Bentonite impregnated TiO2 beads for wastewater treatment *Journal of Photochemistry and Photobiology A: Chemistry*, 412: 113215.

Dhiman, J, Prasher, SO, ElSayed, E, Patel, RM, Nzediegwu, Ch & Mawof, A 2020, Heavy metal uptake by wastewater irrigated potato plants grown on contaminated soil treated with hydrogel based amendments. *Environmental Technology & Innovation*, 19:100952.

Freundlich, HW 1939, The Adsorption of cis- and trans-Azobenzene *Journal of the American Chemical Society*, 1939. 61: 2228-2230.

Gulin Selda Pozan, AK 2014, Significant enhancement of photo catalytic activity over bifunctional ZnO-TiO$_2$ catalysts for 4-chlorophenol degradation. *Chemosphere*, 105: 152-159.

Jawad, MA & Radia, ND 2021, Role of Sodium Alginate-g-poly (Acrylic acid-fumaric acid) Hydrogel for Removal of Pharmaceutical Paracetamol from Aqueous Solutions by Adsorption International *Journal of Pharmaceutical Quality Assurance*, 12: 202-205.

Jiang, W, Guo, X, Yang, M, Lu, Y, Wang, Y, Zheng, Y & Wei, G 2019, Adsorption of cationic dye from water using an iron oxide/activated carbon magnetic composites prepared from sugarcane bagasse by microwave method. *Environmental Technology*, 2 p. DOI: 10.1080/09593330.

Jun, LY, Yon, LS, Mubarak, NM, Bing, ChH, Pan, Sh, Danquah, MK, Abdullah, EC & Khalid, M 2019, An overview of immobilized enzyme technologies for dye and phenolic removal from wastewater. *Journal of Environmental Chemical Engineering*, 7:102961.

Kamil, AM, Mohammed, HT, Alkaim, AF & Hussein, FH 2016, Adsorption of Congo red on multiwall carbon nanotubes: Effect of operational parameters. *Journal of Chemical and Pharmaceutical Sciences*, 9: 1128-1133.

Karimi Maleh, H, Tahernejad Javazmi, F, Gupta, VK, Ahmar, H, Asadi, MH 2020, A novel biosensor for liquid phase determination of glutathione and amoxicillin in biological and pharmaceutical samples using a ZnO/CNTs nanocomposite/catechol derivative modified electrode. *Journal of Molecular Liquids*, 196: 258-263.

Kevadiya, BD, Joshi, GhV, Mody, HM & Hari, C 2021, Bajaj Biopolymer–clay hydrogel composites as drug carrier: Host–guest intercalation and in vitro release study of lidocaine hydrochloride. *Applied Clay Science,* 52: 364-367.

Kim, YS & Kim, JH 2019, Isotherm, kinetic and thermodynamic studies on the adsorption of paclitaxel onto Sylopute. *The Journal of Chemical Thermodynamics*, 130: 104-113.

Kumar, NS, Poulose, AM, Suguna, M & Al Hazza, MI 2019, Equilibrium and kinetic studies of biosorptive removal of 2,4,6-trichlorophenol from aqueous solutions using untreated agro-waste pine cone biomass. *Processes*, 1: 22-33.

Langmuir, I 1918, The adsorption of gases on plane surfaces of glass, mica and platinum. *Journal of the American Chemical Society*, 40: 1361-1403.

Liu, Y, Chen, Y, Yahui Shi, Y, Wan, D, Chen, J & Xiao, Sh 2019, Adsorption of toxic dye Eosin Y from aqueous solution by clay/carbon composite derived from spent bleaching earth. *Journal of Hazardous Materials*, 1: 4656-5544.

Luo, Q, Ren, T, Lei, Z, Huang, Y, Huang, Y, Xu, D, Wan, C, Guo, X & Wu, Y 2022, Non-toxic chitosan-based hydrogel with strong adsorption and sensitive detection abilities for tetracycline *Chemical Engineering Journal,* 427: 131738.

Malatji, N, Makhado, E, Modibane, KD, Ramohlola, KE, Maponya, TC, Monama, GR & Hato, MJ 2021, Removal of methylene blue from wastewater using hydrogel nanocomposites: A review. *Nanomaterials and Technologies for Environmental Applications,* 11: 1-27.

Mittal, H & Ray, SS 2019, A study on the adsorption of methylene blue onto gum ghatti/TiO$_2$ nanoparticles-based hydrogel nanocomposite. *International Journal of Biological Macromolecules*, 88: 66-80.

Mittal, H, Alili, AA, Morajkar, PP & Alhassan, SM 2021, Graphene oxide crosslinked hydrogel nanocomposites of xanthan gum for the adsorption of crystal violet dye. *Journal of Molecular Liquids,* 323: 115034.

Moussavi, G, Alahabadi, A,Yaghmaeian, K, Eskandari, M 2020, Preparation, characterization and adsorption potential of the NH4Cl-induced activated carbon for the removal of amoxicillin antibiotic from water. *Chemical Engineering Journal*, 217: 119-128.

Nasseh, N, Barikbin, B,Taghavi, L & Nasseri, MA 2019, Adsorption of metronidazole antibiotic using a new magnetic nanocomposite from simulated wastewater (isotherm, kinetic and thermodynamic studies). Composites Part B: *Engineering*, 159: 146-156.

Osman, AM, Hendi, AH & Saleh, TA 2020, Simultaneous adsorption of dye and toxic metal ions using an inter-facially polymerized silica/polyamide nanocomposite: Kinetic and thermodynamic studies. *Journal of Molecular Liquids*, 314: 113640.

Sakin, O, Mohmmad, AH, Belal, HM & Arbi, M 2019, Adsorption thermodynamics of cationic dyes (methylene blue and crystal violet) to a natural clay mineral from aqueous solution between 293.15 and 323.15 K. *Arabian Journal of Chemistry*, 11: 615-623.

Tariq, J. AlMusawi, NM, Taghavi, M, Mohebi, S & Balarak, D 2021, Activated carbon derived from Azolla fliculoides fern: a high adsorption capacity adsorbent for residual ampicillin in pharmaceutical wastewater. *Biomass Conversion and Biorefinery*, https://doi.org/10.1007/s13399-021-01962-4.

Thakur, S 2017, Synthesis, characterization and adsorption studies of an acrylic acid-grafted sodium alginate-based TiO_2 hydrogel nanocomposite. *Adsorption Science & Technology*, 36(1-2): 458-477, DOI: 10.1177/0263617417700636

Xiong, J *et al.* 2020, Hexagonal boron nitride adsorbent: Synthesis, performance tailoring and applications. *Journal of Energy Chemistry*, 40: 99-111.

Yasin, AS, Kim, DH & Lee, K 2021, One-pot synthesis of activated carbon decorated with ZnO nanoparticles for capacitive deionization application. *Journal of Alloys and Compounds*, 870: 159422.

Ying, Zh, Yu, Ch, Jian, Zh, Zongrui, T & Shaohua, J 2020, Preparation of SA-g-(PAA-co-PDMC) polyampholytic superabsorbent polymer and its application to the anionic dye adsorption removal from effluents. *Ultrasonics Sonochemistry,* 5: 12-18.

Yu, F, Li, Y, Han, Sh & Jie, M 2019, Adsorptive removal of antibiotics from aqueous solution using carbon materials. *Chemosphere*, 153: 365-385.

Zaheer, Z, Al Asfar, A & Aazam, E 2019, Adsorption of methyl red on biogenic Ag@Fe nanocomposite adsorbent: Isotherms, kinetics and mechanisms. *Journal of Molecular Liquids*, 283: 287-298.

Zhao, Sh, Zhan, Y, Wan, X, SHe, SH,Yang, X, JHu, J & Zhang, G 2020, Selective and efficient adsorption of anionic dyes by core/shell magnetic MWCNTs nano-hybrid constructed through facial polydopamine tailored graft polymerization: Insight of adsorption mechanism, kinetic, isotherm and thermodynamic study. *Journal of Molecular Liquids*, 319: 1-6.